Astronomy & Astrophysics manuscript no. ripa˙aa
February 10, 2009

Search for Gamma-Ray Burst Classes with the RHESSI Satellite

J. Řípa[1], A. Mészáros[1], C. Wigger[2,4], D. Huja[1], R. Hudec[3], and W. Hajdas[2]

[1] Charles University, Faculty of Mathematics and Physics, Astronomical Institute, V Holešovičkách 2, CZ 180 00 Prague 8, Czech Republic
e-mail: ripa@sirrah.troja.mff.cuni.cz
e-mail: meszaros@cesnet.cz
e-mail: David.HUJA@seznam.cz
[2] Paul Scherrer Institute, CH-5232 Villigen, Switzerland
e-mail: wojtek.hajdas@psi.ch
e-mail: claudia.wigger@kanti-wohlen.ch
[3] Astronomical Institute, Academy of Sciences of the Czech Republic, CZ 251 65 Ondřejov, Czech Republic
e-mail: rhudec@asu.cas.cz
[4] Kantonsschule Wohlen, 5610 Wohlen, Switzerland

Received September 04, 2008; accepted February 02, 2009

ABSTRACT

Aims. A sample of 427 gamma-ray bursts (GRBs), measured by the RHESSI satellite, is studied statistically with respect to duration and hardness ratio.
Methods. Standard statistical tests are used, such as χ^2, F-test and the maximum likelihood ratio test, in order to compare the number of GRB groups in the RHESSI database with that of the BATSE database.
Results. Previous studies based on the BATSE Catalog claim the existence of an intermediate GRB group, besides the long and short groups. Using only the GRB duration T_{90} as information and χ^2 or F-test, we have not found any statistically significant intermediate group in the RHESSI data. However, maximum likelihood ratio test reveals a significant intermediate group. Also using the 2-dimensional hardness / T_{90} plane, the maximum likelihood analysis reveals a significant intermediate group. Contrary to the BATSE database, the intermediate group in the RHESSI data-set is harder than the long one.
Conclusions. The existence of an intermediate group follows not only from the BATSE data-set, but also from the RHESSI one.

Key words. gamma-rays: bursts

1. Introduction

In the years 1991 – 2000 cca 3000 gamma-ray bursts (GRBs) were detected by the BATSE instrument on board the Compton Gamma-Ray Observatory (Meegan et al. 2001). After the end of this mission (June 2000) the number of discovered GRBs decreased (down to ∼ 100 – 200 GRBs annually) due to different observational methods on the operating satellites. Any observational GRB database from the period 2000 and latter, can have a great importance. Such important GRB observations are records obtained by the RHESSI satellite (Holman et al. 2008) ∼ 70/year.

Originally it was found (Kouveliotou et al. 1993) that there exist two GRB classes: the short one with durations $\lesssim 2$ s and the long one with durations $\gtrsim 2$ s. This was confirmed with GRB data from the Konus-Wind instrument (Aptekar et al. 1998). However, some articles point to the existence of three classes of GRBs in the BATSE database with respect to their durations (Horváth 1998, Horváth 2002). The work Horváth et al. (2008), using maximum likelihood ratio test on durations, gives that there is a statistically significant intermediate group in the Swift data-set. Also Horváth et al. (2004) and Horváth et al. (2006) claimed that, when using a 2-dimensional plane of hardness ratio vs. duration, three classes of GRBs can be found in the BATSE data-set. Mukherjee et al. (1998) pointed to the existence of three GRB classes in multiparameter space. In another multidimensional analysis of the BATSE catalog by Chattopadhyay et al. (2007) it is argued that at least three clusters of GRBs are found. Some articles also say that the third class (with intermediate duration), observed by BATSE, is a bias caused by an instrumental effect (Hakkila et al. 2000). In Hakkila et al. (2004) there is a review and discussion of GRB classifying, based on statistical clustering and data mining techniques, placing the intermediate group as a separate source population in doubt.

The purpose of this paper is to investigate the number of GRB groups in another data set, namely in the GRB data set provided by the RHESSI satellite. Although the main goal of the RHESSI satellite is the study of solar physics, it has a useful set of GRB observations also covering the period 2002 – 2004. Hence its study can be maximally useful. Trivially, any comparison of different catalogs using different instruments is useful for an independent confirmation of previous results.

In the first step the 1-dimensional duration distribution of GRBs observed by RHESSI is analysed, and in the second step the two-dimensional plane of hardness ratio vs. duration is used. In order to determine the number of GRB groups, standard statistical tests described in Trumpler & Weaver (1953), Press et al. (1992), Zey et al. (2006) are used.

Send offprint requests to: J. Řípa

The paper is organized as follows: in section 2, the RHESSI satellite and the analysed data-set are described. In section 3, we present the duration distribution for the RHESSI GRBs and its analysis. In section 4, the 2-dimensional hardness ratio vs. duration distribution and the maximum likelihood fit of these data are presented. In sections 5 and 6, the discussion and conclusion follow. At the end, the RHESSI data-sample is listed.

2. The RHESSI Data Sample

The Ramaty High Energy Solar Spectroscopic Imager (RHESSI) is a NASA Small Explorer satellite designed to study hard X-rays and gamma-rays from solar flares (Lin et al. 2002). It consists mainly of an imaging tube and a spectrometer. The spectrometer consists of nine germanium detectors (7.1 cm in diameter and a height of 8.5 cm) (Smith et al. 2002). They are only lightly shielded, thus making RHESSI also very useful to detect non-solar photons from any direction (Smith et al. 2003). The energy range for GRB detection extends from about 30 keV up to 17 MeV. Over a wide range of energies and GRB incoming directions, the effective area is around 150 cm^2 (Wigger et al. 2006b). With a field of view of about half of the sky, RHESSI observes about one or two GRBs per week. Photon hits are stored event-by-event in onboard memory with a time sampling of $\Delta t = 1\,\mu$s resolution. The energy resolution for lines is excellent: $\Delta E = 3$ keV at 1000 keV.

We used the RHESSI GRB Catalog (Wigger et al. 2008) and the Cosmic Burst List (Hurley 2008) to find 487 GRBs in the RHESSI data between the 14^{th} February 2002 and 25^{th} April 2008. We should mention the strategy how RHESSI GRBs are found. There is no automatic GRB search routine. Only if there is a message from any other instrument of the IPN (Hurley 2007), the RHESSI data are searched for a GRB signal. Therefore, in our data-set there are only GRBs, which are also observed by other instruments. The biggest overlap is with Konus-W. About 85 % of all RHESSI GRBs are also observed by Konus-W (Wigger et al. 2006a).

For a deeper analysis we have chosen a subset of 427 GRBs with a signal/noise ratio better than 6. We have used the SolarSoftWare (Freeland et al. 2008) program running under the Interactive Data Language (RSI IDL) programming application as well as our own IDL routines to derive count light-curves (with the time resolution better than 10 % of the burst's duration for the great majority of our whole data-set) and count fluences from the rear detectors' segments (except number R2) of the RHESSI spectrometer (Smith et al. 2002) in the energy band from 25 keV to 1.5 MeV. This data-set (together with the time resolutions of derived light-curves) are listed in the Table 7 – Table 13.

3. Duration Distribution

First we study the 1-dimensional duration distribution. We use T_{90} as the GRB duration, i.e. the time interval during which the cumulative counts increase from 5 % to 95 % above background (Meegan et al. 2001). The T_{90} uncertainty consists of two components. We make an assumption that one is given by the count fluence uncertainty during T_{90} (δt_s), which is given by Poisson noise, and the second one is the time resolution of derived light-curves (δt_{res}). The total T_{90} uncertainty δt was calculated as $\delta t = \sqrt{\delta t_s^2 + \delta_{res}^2}$.

The histogram of the times T_{90} gives a distribution with two maxima: at approximately 0.2 s and 20 s (Fig. 1.). The histogram consists of 19 equally wide bins on logarithmic scale (with base 10) starting at 0.09 s and ending at 273.4 s.

We follow the method done by Horváth (1998) and fitted one, two (Fig. 1.) and three (Fig. 2.) log-normal functions and used the χ^2 test to evaluate these fits. The minimal number of GRBs per bin is 4 (last bin), hence the use of the χ^2 test is possible.

In the case of the fit with one log-normal function we obtained $\chi^2 \simeq 157$ for 17 degrees of freedom (dof). Therefore, this hypothesis is rejected on a smaller than 0.01 % significance level.

The fit with two log-normal functions is shown in Fig. 1 and the fit with three log-normal functions in Fig. 2. The parameters of the fits, the values of χ^2, the degrees of freedom and the goodness-of-fits are listed in Table 1.

The assumption of two groups being represented by two log-normal fits is acceptable, the fit with three log-normal functions even more. The question is whether the improvement in χ^2 is statistically significant. To answer this question, we used the F-test, as described by Band et al. (1997), Appendix A. The F-test gives a probability of 6.9 % of the improvement in χ^2 being accidental. This value is remarkably low, but not low enough to reject the hypothesis that two log-normal functions are still enough to describe the observed duration distribution.

In order to know how the T_{90} uncertainties effect our result, we randomly picked up one half of the bursts and shifted their durations by the full amount of their uncertainties to lower values and the second half to higher values. Then we made a histogram and recalculated the best fitted parameters, χ^2 and F-test. The results for ten such calculations are listed in the Table 2. This method also gives us information how the fitted parameters vary, and thus tells what are their uncertainties. From Table 2 we see that, on average, the improvement in χ^2 is not significant. Therefore, we can not proclaim acceptance of three groups by using this statistical method.

Since the number of GRBs is low for many bins, we also used the maximum likelihood method (see Horváth 2002 and the references therein) in order to fit two and three log-normal functions on the RHESSI data-set.

The parameters are listed in the Table 3.

As the difference of the logarithms of the likelihoods $\Delta \ln L = 9.2$ should be half of the χ^2 distribution for 3 degrees of freedom (Horváth 2002), we obtain that the introduction of a third group is statistically significant on the 0.036 % level (of being accidental).

To get an image how T_{90} uncertainties effect our result, we proceed similarly as in the χ^2 fitting and generated ten different data-sets randomly changed in durations by the full amount of their uncertainties. The results are presented in the Table 4. From this table it is seen that all ten simulations give probabilities, that introducing of the third group is accidental, much lower than 5 %. Thus, the hypothesis of introducing third group is highly acceptable.

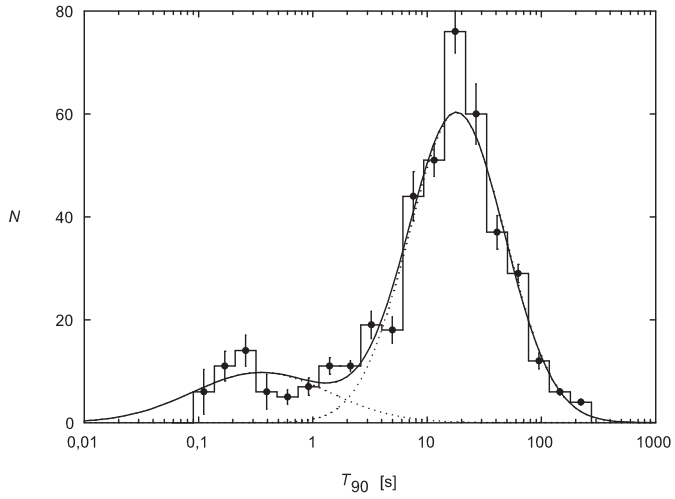

Fig. 1. Duration distribution of the 427 RHESSI bursts with the best χ^2 fit of two log-normal functions. Number of bins is 19, $dof = 14$ and $\chi^2 \simeq 19.1$ which implies the goodness-of-fit $\simeq$ 16 %. The bar errors are standard deviations of the number of GRBs per bin for ten different simulated duration distributions as described in the text.

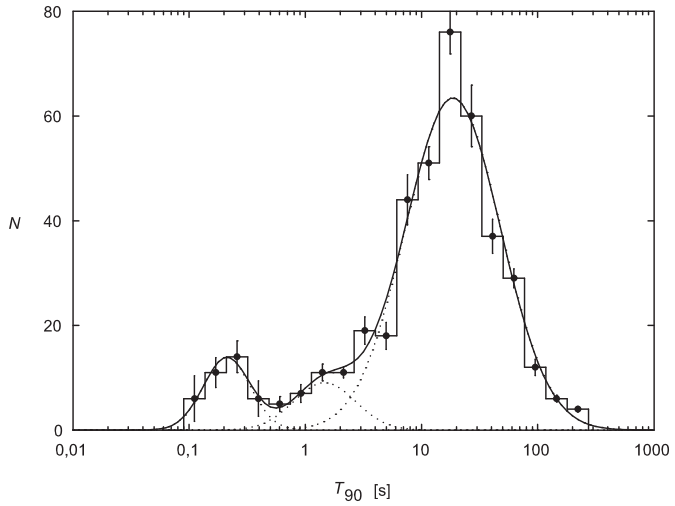

Fig. 2. Duration distribution of the 427 RHESSI bursts with the best χ^2 fit of three log-normal functions. Number of bins is 19, $dof = 11$ and $\chi^2 \simeq 10.3$ which implies the goodness-of-fit $\simeq$ 50 %. The bar errors are the same as described in Fig. 1.

4. Hardness Ratio vs. Duration

A two-dimensional scatter plot of RHESSI GRBs is shown in Fig. 3 and Fig. 4. One axis is the duration T_{90}, used in the previous section, the other axis is a hardness ratio. The hardness ratio is defined as a ratio of two fluences F in two different energy bands integrated over the time interval T_{90}. For the RHESSI data-set, we used the energy bands (25 – 120) keV and (120 – 1500) keV, i.e. $H = F_{120-1500}/F_{25-120}$.

Using the maximum likelihood method (see Horváth et al. (2004), Horváth et al. (2006) and the references therein), we fit two and three bivariate log-normal functions in order to search for clusters. In Fig. 3., we show the best fit of two bivariate log-normal functions (11 independent parameters, since the two weights must add up to 100 %).

Table 1. Parameters of the best χ^2 fits of two and three log-normal functions on the RHESSI GRB T_{90} distribution. μ are the means, σ are the standard deviations and w are the weights of the distribution. Given uncertainties are standard deviations of the parameters obtained by ten different fittings of randomly changed histogram of durations by their uncertainties.

parameter	2 log-normal	3 log-normal
$\mu_{\rm short}$	-0.46±0.13	-0.68±0.09
$\sigma_{\rm short}$	0.60±0.06	0.20±0.03
$w_{\rm short}$[%]	18.7±1.5	8.9±1.0
$\mu_{\rm long}$	1.26±0.03	1.27±0.03
$\sigma_{\rm long}$	0.42±0.01	0.41±0.01
$w_{\rm long}$[%]	81.3±1.5	83.4±0.9
$\mu_{\rm middle}$		0.17±0.06
$\sigma_{\rm middle}$		0.27±0.06
$w_{\rm middle}$[%]		7.7±1.0
dof	14	11
χ^2	19.13	10.30
goodness[%]	16.0	50.4
F_0	3.14	
$P(F > F_0)$[%]	6.9	

Table 2. The minimal χ^2, corresponding goodness-of-fits and F-tests for fitted two and three log-normal functions on the RHESSI GRB T_{90} distribution for ten different changes of durations by their uncertainties.

2 log-normal		3 log-normal		F-test
χ^2	goodness [%]	χ^2	goodness [%]	$P(F > F_0)$ [%]
23.97	4.6	14.19	22.3	11.1
18.03	20.6	10.65	47.3	11.0
15.99	31.4	5.13	92.5	0.5
13.52	48.6	7.50	75.8	8.0
17.87	21.3	7.55	75.3	2.0
16.36	29.2	9.66	56.1	11.0
11.89	61.5	6.95	80.3	10.4
21.86	8.2	13.77	24.6	15.1
20.07	12.8	9.49	57.7	3.5
20.40	11.8	12.73	31.1	14.4

The parameters are listed in Table 5. One result is that the short GRBs are on average harder than long GRBs. Having a closer look at the GRB distribution within the short class, one can see that the points within the 1σ ellipse are not evenly distributed. They cluster towards the shortest durations (Fig. 3).

The fitting with the sum of three groups (17 independent parameters) is shown in Fig. 4. The fitted parameters are listed in Table 5. The former short group is clearly separated into two parts. As far as one can tell by sight, the data points scatter evenly within (and around) the 1σ ellipses.

As the difference of the logarithms of the likelihoods $\Delta \ln L = 10.9$ should be half of the χ^2 distribution for 6 degrees

Table 3. Parameters of the best fit with two and three log-normal functions done by the maximum likelihood method on the RHESSI data. μ are the means, σ are the standard deviations, w are the weights of the distribution and L_2, L_3 are the likelihoods. Given uncertainties are standard deviations of the parameters obtained by ten different fittings of data-sets, in which the durations were randomly changed by their uncertainties.

parameter	2 log-normal	3 log-normal
$\mu_{\rm short}$	-0.60±0.07	-0.64±0.02
$\sigma_{\rm short}$	0.25±0.05	0.20±0.02
$w_{\rm short}$[%]	10.2±1.3	9.4±0.4
$\mu_{\rm long}$	1.20±0.01	1.26±0.01
$\sigma_{\rm long}$	0.47±0.01	0.41±0.01
$w_{\rm long}$[%]	89.8±1.3	84.4±1.0
$\mu_{\rm middle}$		0.17±0.04
$\sigma_{\rm middle}$		0.22±0.06
$w_{\rm middle}$[%]		6.2±1.4
$\ln L_2$	-389.17	
$\ln L_3$		-379.95

Table 4. The maximal likelihoods and corresponding probabilities that introducing of the third group is accidental for maximum likelihood fittings (one-dimensional) with two and three log-normal functions of ten different changes of durations by their uncertainties.

$\ln L_2$	$\ln L_3$	probability [%]
-388.12	-378.86	0.03
-390.82	-383.92	0.32
-391.90	-380.97	0.01
-391.75	-385.37	0.52
-392.25	-384.24	0.11
-390.62	-383.67	0.30
-386.26	-375.54	0.01
-392.33	-384.97	0.21
-389.16	-380.93	0.09
-390.21	-384.32	0.82

of freedom (Horváth et al. 2006), we obtain that the introduction of a third group is statistically significant on the 0.13 % level (of being accidental).

To get an image how GRB durations and hardness ratio uncertainties effect our result, we proceed similarly as in the χ^2 fitting and generated ten different data-sets randomly changed in durations and hardness ratios by the full amount of their uncertainties. The results are presented in the Table 6. From this table it is seen that almost all simulations give probabilities, that introducing of the third group is accidental, much lower than 5 %. Thus, the hypothesis of introducing the third group is highly acceptable.

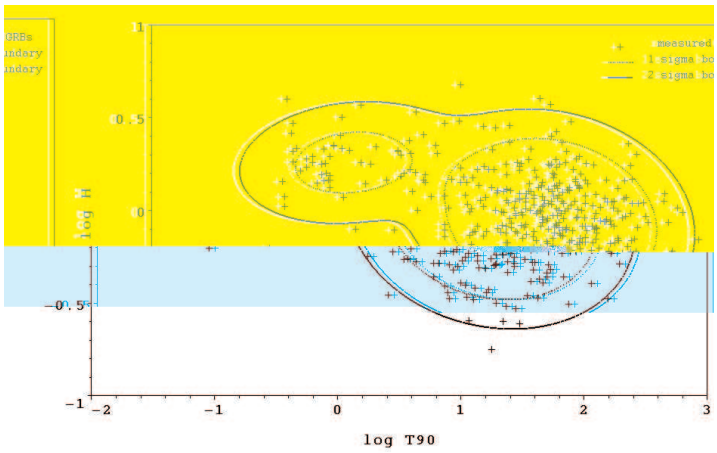

Fig. 3. Hardness ratio vs. T_{90} of the RHESSI GRBs with the best fit of two bivariate log-normal functions.

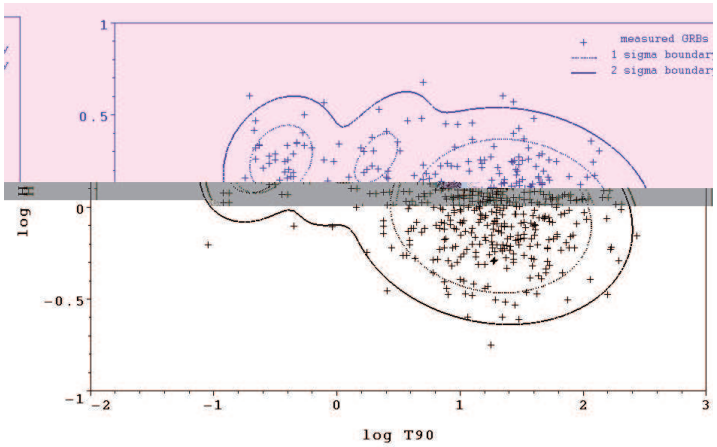

Fig. 4. Hardness ratio vs. T_{90} of the RHESSI GRBs with the best fit of three bivariate log-normal functions.

5. Discussion

The analysis of the 1-dimensional duration distribution, by the χ^2 fitting, reveals the class of so called long GRBs (about 83 % of all RHESSI GRBs) with typical durations from 5 to 70 seconds, the most probable duration being $T_{90} \approx 19$ s. Another class are short GRBs (about 9 % of all RHESSI GRBs) with typical durations from 0.1 to 0.4 seconds, the most probable duration being $T_{90} \approx 0.21$ s. By fitting 3 log-normal functions we find a third class (about 8 % of all RHESSI GRBs) with typical durations from 0.8 to 3 seconds, the most probable duration being $T_{90} \approx 1.5$ s. The existence of the intermediate class from the RHESSI T_{90} distribution is not confirmed on a sufficiently high significance using only the χ^2 fit. However, the maximum likelihood ratio test on the same data reveals that the introduction of a third class is statistically significant. The χ^2 method might not be as much sensitive and hance decisive as the likelihood method, because of the low number of bursts in our data-sample (Horváth et al. 2008, 2^{nd} section, 1^{st} paragraph).

The hardness ratio vs. duration plot for the RHESSI sample does further demonstrate the existence of a third class. The typical durations are very similar to the ones obtained with the 1-dimensional analysis, the percentages are slightly different (≈ 86 % long, ≈ 9 % short, ≈ 5 % intermediate).

Three classes of GRBs were also reported for the BATSE GRBs (Horváth et al. 2006) and the Swift GRBs

Table 5. Parameters of the best fit with two and three bivariate log-normal functions done by the maximum likelihood method on the RHESSI data. $\mu_{\rm x}$ are the means on the x-axis ($x = \log T_{90}$), $\mu_{\rm y}$ are the means on the y-axis ($y = \log H$), $\sigma_{\rm x}$ are the dispersions on the x-axis, $\sigma_{\rm y}$ are the dispersions on the y-axis, r are the correlation coefficients, w are the weights of the distribution and L_2, L_3 are the likelihoods. Given uncertainties are standard deviations of the parameters obtained by ten different fittings of data-sets, where the durations and hardness ratios were randomly changed by their uncertainties.

parameter	2 log-normal	3 log-normal
$\mu_{\rm x,short}$	-0.38±0.018	-0.65±0.018
$\mu_{\rm y,short}$	0.26±0.010	0.26±0.009
$\sigma_{\rm x,short}$	0.42±0.012	0.20±0.016
$\sigma_{\rm y,short}$	0.15±0.009	0.15±0.012
$w_{\rm short}$[%]	14.2±0.3	9.2±0.5
$r_{\rm short}$	0.14±0.092	0.22±0.119
$\mu_{\rm x,long}$	1.25±0.004	1.25±0.006
$\mu_{\rm y,long}$	-0.05±0.004	-0.05±0.004
$\sigma_{\rm x,long}$	0.42±0.004	0.42±0.005
$\sigma_{\rm y,long}$	0.22±0.003	0.22±0.003
$w_{\rm long}$[%]	85.8±0.3	85.5±0.8
$r_{\rm long}$	-0.14±0.018	-0.13±0.020
$\mu_{\rm x,middle}$		0.11±0.029
$\mu_{\rm y,middle}$		0.27±0.019
$\sigma_{\rm x,middle}$		0.21±0.057
$\sigma_{\rm y,middle}$		0.17±0.035
$w_{\rm middle}$[%]		5.3±1.1
$r_{\rm middle}$		0.59±0.230
$\ln L_2$	-323.91	
$\ln L_3$		-313.00

Table 6. The maximal likelihoods and corresponding probabilities that introducing of the third group is accidental for maximum likelihood fittings (two-dimensional) with two and three bivariate log-normal functions of ten different changes of durations and hardness ratios by their uncertainties.

$\ln L_2$	$\ln L_3$	probability [%]
-349.40	-339.92	0.42
-348.28	-336.36	0.06
-350.66	-340.80	0.31
-347.12	-338.15	0.64
-349.64	-340.47	0.54
-344.59	-338.17	4.56
-350.36	-342.47	1.50
-344.44	-334.71	0.35
-349.37	-336.51	0.03
-348.06	-338.57	0.42

(Horváth et al. 2008). For BATSE, ≈ 65 % of all GRBs are long, ≈ 24 % short and ≈ 11 % intermediate (Horváth et al. 2006 Table 2. of that article). The typical durations found for BATSE are roughly a factor 2 longer than for RHESSI, but consistent for all three classes. As is known from BATSE, also in the RHESSI data-set, the short GRBs are on average harder than the long GRBs. The most remarkable difference is the hardness of the intermediate class. In the BATSE data, the intermediate class has the lowest hardness ratio, which is anti-correlated with the duration (Horváth et al. 2006), whereas we find for the RHESSI data that its hardness is comparable with that of the short group and correlated with the duration, but this correlation is not conclusive because of its large error. The hardness of the intermediate class found with RHESSI is surprising since the intermediate class in the BATSE data was found to be the softest. This discrepancy might by explained by the different definitions of the hardnesses. The hardness H for the RHESSI data is defined as $H = F_{120-1500}/F_{25-120}$, whereas for the BATSE data $H = F_{100-320}/F_{50-100}$, where the numbers denotes energy in keV (the BATSE fluences at higher energies than 320 keV are noisy (Bagoly et al. 1998)). This means that hardnesses do not measure the same bursts' behaviours. Even more different is the situation if we compare hardnesses in the Swift and RHESSI databases, because the Swifts' hardnesses are defined as $H = F_{100-150}/F_{50-100}$ and $H = F_{50-100}/F_{25-50}$ (Horváth et al. 2008, Sakamoto et al. 2008).

The shorter durations of the RHESSI GRBs compared to the BATSE GRBs can be understood: For RHESSI, which is practically unshielded, the background is high (minimum around 1000 counts per second in the (25 – 1500) keV band) and varies by up to a factor 3. Additionally, RHESSI's sensitivity drops rapidly below ≈ 50 keV. Weak GRBs (in the sense of counts per second) and soft GRBs are not so well observed by RHESSI. Since GRBs tend to be softer and weaker at later times, they will sooner fall beyond RHESSI's detection limit, resulting in a shorter duration.

For Swift, ≈ 58% of all GRBs are long, ≈ 7% short and ≈ 35% intermediate (Horváth et al. 2008). The percentage of each group depends obviously on the instrument.

6. Conclusion

The RHESSI data confirm that GRBs can be separated into a short and long class, and that the short GRBs are on average harder than the long ones. The two-dimensional analysis in the hardness/duration plane as well as the maximum likelihood fit of the duration distribution show a third class with intermediate duration and similar hardness as the short class.

Acknowledgements. This study was supported by the GAUK grant No. 46307, by the OTKA grants No. T48870 and K 77795, by the Grant Agency of the Czech Republic grant No. 205/08/H005, by the Research Program MSM0021620860 of the Ministry of Education of the Czech Republic, by the INTEGRAL PECS Project 98023 and by the grant GA ČR 205/08/1207. We appreciate help of K. Hurley with the RHESSI GRB list, valuable discussion with L.G. Balázs and useful remarks of O. Wigger. Thanks are due to the anonymous referee for the worthwhile notes.

References

Aptekar, R.L., et al. 1998, AIPC, 428, 10
Band, D.L., et al. 1997, ApJ, 485, 747, Appendix A
Bagoly, Z., et al. 1998, ApJ, 498, 342
Chattopadhyay, T., et al. 2007, ApJ, 667, 1017
Freeland, S.L., et al. 2008, http://www.lmsal.com/solarsoft
Hakkila, J., et al. 2000, ApJ, 538, 165
Hakkila, J., et al. 2004, Baltic Astronomy, 13, 211
Holman, G.D. 2008, http://hesperia.gsfc.nasa.gov/hessi
Horváth, I. 1998, ApJ, 508, 757
Horváth, I. 2002, A&A, 392, 791
Horváth, I., et al. 2004, Baltic Astronomy, 13, 217
Horváth, I., et al. 2006, A&A, 447, 23
Horváth, I., et al. 2008, A&A, 489, L1

Hurley, K. 2007, http://www.ssl.berkeley.edu/ipn3/index.html
Hurley, K. 2008, http://www.ssl.berkeley.edu/ipn3/masterli.html
Kouveliotou, C., et al. 1993, ApJ, 413, 101
Lin, R.P., et al. 2002, Solar Physics, 210, 3
Meegan, C.A., et al. 2001, Current BATSE Gamma-Ray Burst Catalog, http://gammaray.msfc.nasa.gov/batse/grb/catalog
Mukherjee, S., et al. 1998, ApJ, 508, 314
Press, W.H., et al. 1992, Numerical Recipes in C, Cambridge University Press
RSI IDL, http://rsinc.com/idl/
Sakamoto, T., et al. 2008, ApJS, 175, 179
Smith, D.M., et al. 2002, Solar Physics, 210, 33
Smith, D.M., et al. 2003, Proceedings of SPIE Vol. 4851, 1163
Trumpler, R.J. & Weaver, H.F. 1953, Statistical Astronomy, University of California Press, Berkeley
Wigger, C., et al. 2006, http://grb.web.psi.ch/publications/talk_venice.pdf
Wigger, C., et al. 2006, Il Nuovo Cimento, 121 B, N. 10-11, 1117
Wigger, C., et al. 2008, http://grb.web.psi.ch
Zey, C, et al. NIST/SEMATECH, e-Handbook of Statistical Methods, http://www.itl.nist.gov/div898/handbook/, 2006

Table 7. The RHESSI GRB data-set including I. GRB names which correspond to dates (the letters after GRB names are internal and do not have to be in accordance with e.g. GCN GRB names), II. GRB peak time, III. T_{90} duration, IV. time resolution δt_{res} (described above) and V. hardness ratios.

GRB	peak time UTC	T_{90} [s]	δt_{res} [s]	hardness ratio log H
020214	18:49:47.700	(1.42±0.03)E+1	2.0E-1	(6.03±0.16)E-1
020218	19:49:41.750	(3.40±0.06)E+1	5.0E-1	-(1.12±0.11)E-1
020302	12:23:54.400	(4.88±0.32)E+1	8.0E-1	(1.65±0.53)E-1
020306	18:58:02.893	(1.35±0.16)E-1	1.5E-2	(4.16±0.40)E-1
020311	01:21:31.550	(1.08±0.06)E+1	3.0E-1	(6.55±3.88)E-2
020313	01:17:53.400	(2.32±0.10)E+1	4.0E-1	-(5.17±0.50)E-1
020315	15:42:47.550	(1.26±0.11)E+1	3.0E-1	(2.97±6.94)E-2
020331	10:23:26.750	(3.90±0.53)E+1	5.0E-1	-(0.46±1.05)E-1
020407	04:14:44.300	(2.10±0.09)E+1	6.0E-1	-(1.72±2.76)E-2
020409	09:27:23.500	(1.46±0.14)E+2	1.0E+0	(8.84±7.37)E-2
020413	16:20:15.500	(9.00±0.64)E+0	2.0E-1	-(2.89±5.57)E-2
020417	05:36:26.250	(7.85±0.52)E+1	5.0E-1	-(1.62±0.58)E-1
020418	17:43:08.850	(3.40±0.13)E+0	1.0E-1	(1.81±0.20)E-1
020426	23:56:14.795	(1.20±0.32)E-1	3.0E-2	(7.40±7.13)E-2
020430	21:22:01.650	(1.35±0.05)E+1	3.0E-1	-(2.73±0.32)E-1
020509	00:01:17.675	(3.50±0.38)E+0	5.0E-2	(8.32±8.52)E-2
020524	02:12:47.300	(1.48±0.08)E+1	2.0E-1	(7.46±4.26)E-2
020525A	03:47:53.650	(7.60±0.61)E+0	1.0E-1	(1.10±0.65)E-1
020525B	04:26:53.210	(1.80±0.29)E-1	2.0E-2	(2.78±0.96)E-1
020527	05:17:20.525	(1.65±0.18)E+0	5.0E-2	(1.94±0.88)E-1
020602	17:30:28.085	(1.75±0.19)E+0	7.0E-2	-(2.49±0.91)E-1
020603	17:50:34.905	(1.44±0.06)E+0	3.0E-2	-(0.07±3.08)E-2
020604	14:13:42.850	(7.20±0.41)E+0	3.0E-1	-(1.37±3.19)E-2
020620	12:58:06.875	(3.45±0.22)E+0	5.0E-2	-(2.63±0.56)E-1
020623	04:23:07.350	(6.60±0.46)E+0	1.0E-1	-(2.84±0.66)E-1
020630	07:58:52.650	(3.30±0.26)E+1	3.0E-1	-(1.48±0.66)E-1
020702	15:54:16.250	(3.69±0.24)E+1	3.0E-1	-(3.85±0.71)E-1
020708	04:34:12.500	(2.70±0.40)E+1	1.0E+0	-(3.00±1.29)E-1
020712	06:09:44.100	(1.80±0.20)E+1	2.0E-1	-(1.51±0.93)E-1
020715A	15:14:26.735	(2.40±0.40)E-1	3.0E-2	(1.92±0.88)E-1
020715B	19:21:09.100	(6.40±0.21)E+0	2.0E-1	(1.05±0.10)E-1
020725	16:25:41.150	(5.00±0.31)E+0	1.0E-1	(2.37±0.51)E-1
020801	11:52:41.550	(1.43±0.09)E+1	1.0E-1	-(8.54±5.30)E-2
020819A	07:56:39.455	(1.05±0.08)E+0	3.0E-2	(1.85±0.60)E-1
020819B	14:57:38.600	(9.20±0.75)E+0	4.0E-1	-(2.13±0.64)E-1
020828	05:45:37.925	(6.60±0.45)E-1	3.0E-2	(3.41±0.48)E-1
020910	19:57:43.150	(2.85±0.10)E+1	3.0E-1	(1.33±0.29)E-1
020914	21:53:20.100	(1.08±0.09)E+1	2.0E-1	-(2.54±0.73)E-1
020926	04:52:54.200	(2.24±0.15)E+1	8.0E-1	-(2.05±0.53)E-1
021008A	07:01:03.550	(1.45±0.01)E+1	1.0E-1	(1.34±0.03)E-1
021008B	14:30:04.500	(1.42±0.12)E+1	2.0E-1	(0.09±6.92)E-2
021011	04:38:11.250	(5.10±0.32)E+1	5.0E-1	-(2.94±0.61)E-1
021016	10:29:43.500	(8.30±0.54)E+1	1.0E+0	-(1.54±0.55)E-1
021020	20:12:57.350	(1.44±0.04)E+1	3.0E-1	-(0.64±1.86)E-2
021023	02:53:47.300	(1.36±0.05)E+1	2.0E-1	-(0.60±2.85)E-2
021025	20:18:30.150	(1.86±0.22)E+1	3.0E-1	-(1.22±0.95)E-1
021102	15:58:31.850	(1.08±0.05)E+1	3.0E-1	-(4.04±0.41)E-1
021105	05:27:18.650	(6.40±0.80)E+0	1.0E-1	-(9.92±9.89)E-2
021108	05:39:55.800	(2.20±0.17)E+1	4.0E-1	-(5.99±1.07)E-1
021109	08:42:49.000	(1.96±0.13)E+1	4.0E-1	-(2.87±5.23)E-2
021113	13:37:37.625	(3.98±0.48)E+1	2.5E-1	-(2.82±1.08)E-1
021115	13:33:04.250	(1.26±0.15)E+1	3.0E-1	-(4.79±1.31)E-1
021119	12:54:07.700	(2.82±0.08)E+1	2.0E-1	-(1.83±0.26)E-1
021125	17:58:31.250	(6.75±0.12)E+1	5.0E-1	-(3.57±0.18)E-1
021201	05:30:04.175	(3.40±0.16)E-1	1.0E-2	(4.03±0.36)E-1
021205	03:18:29.750	(7.65±0.33)E+1	1.5E+0	-(2.23±0.36)E-1
021206	22:49:16.650	(4.92±0.02)E+0	2.0E-2	(2.26±0.22)E-2
021211	11:18:35.040	(4.32±0.32)E+0	8.0E-2	-(2.79±0.68)E-1
021214	03:27:25.500	(3.00±0.28)E+1	1.0E+0	-(2.07±0.77)E-1
021223	01:10:00.250	(8.00±0.64)E+0	1.0E-1	-(2.92±0.77)E-1
021226	14:53:39.675	(3.50±0.53)E-1	5.0E-2	(3.34±0.43)E-1
030102	23:18:59.350	(1.32±0.09)E+1	3.0E-1	-(1.65±0.56)E-1

Table 8. The RHESSI GRB data-set.

GRB	peak time UTC	T_{90} [s]	δt_{res} [s]	hardness ratio log H
030103	21:46:46.750	(1.00±0.12)E+1	5.0E-1	-(3.93±1.14)E-1
030105	14:34:11.995	(1.23±0.06)E+0	3.0E-2	(3.77±0.40)E-1
030110	09:39:30.205	(9.00±3.14)E-2	3.0E-2	-(2.04±0.88)E-1
030115A	06:25:37.250	(7.95±0.14)E+1	5.0E-1	(3.54±1.40)E-2
030115B	08:15:48.500	(2.70±0.10)E+1	2.0E-1	-(2.83±0.36)E-1
030127	12:32:42.750	(3.80±0.40)E+1	5.0E-1	(2.34±8.30)E-2
030204	12:45:36.500	(5.60±0.13)E+1	1.0E+0	(1.39±1.34)E-2
030206	11:00:32.010	(1.40±0.24)E-1	2.0E-2	(2.62±0.83)E-1
030212	22:17:18.450	(2.31±0.26)E+1	3.0E-1	-(2.25±0.97)E-1
030214	14:48:21.325	(1.83±0.10)E+1	1.5E-1	-(2.07±0.49)E-1
030216	16:13:44.150	(9.30±1.40)E+0	3.0E-1	-(1.20±1.16)E-1
030217	02:45:42.600	(5.40±0.08)E+1	8.0E-2	(4.46±1.28)E-2
030222	16:32:53.250	(1.44±0.18)E+1	3.0E-1	-(2.01±1.02)E-1
030223	09:45:15.250	(2.05±0.11)E+1	5.0E-1	(2.50±0.42)E-1
030225	15:02:53.750	(2.00±0.11)E+1	5.0E-1	-(9.23±4.20)E-2
030227	13:12:05.250	(7.10±1.03)E+1	5.0E-1	(0.68±1.11)E-1
030228	20:26:47.250	(2.80±0.18)E+1	5.0E-1	-(3.96±4.98)E-2
030301	20:27:21.500	(4.30±0.35)E+1	1.0E+0	-(3.73±0.85)E-1
030306	03:38:16.150	(1.26±0.04)E+1	3.0E-1	-(1.16±0.22)E-1
030307	14:31:58.950	(3.80±0.11)E+0	1.0E-1	-(1.34±0.13)E-1
030320A	10:12:01.150	(4.86±0.15)E+1	3.0E-1	-(6.10±2.51)E-2
030320B	18:49:35.500	(1.56±0.06)E+2	3.0E+0	-(6.38±2.83)E-2
030326	10:43:44.150	(1.26±0.06)E+1	3.0E-1	-(2.01±0.34)E-1
030328	07:28:48.250	(6.55±0.26)E+1	5.0E-1	-(4.09±3.25)E-2
030329A	11:37:40.850	(1.74±0.03)E+1	3.0E-1	-(2.60±0.06)E-1
030329B	15:34:18.500	(6.10±0.29)E+1	1.0E+0	-(1.50±0.39)E-1
030331	05:38:49.500	(2.38±0.11)E+1	2.0E-1	-(3.34±0.47)E-1
030406	22:42:57.450	(7.02±0.13)E+1	3.0E-1	-(3.30±1.54)E-2
030410	11:23:42.275	(1.60±0.16)E+0	5.0E-2	(4.10±1.01)E-1
030413	07:34:45.550	(2.04±0.09)E+1	3.0E-1	(1.48±0.35)E-1
030414	13:48:28.250	(2.85±0.08)E+1	5.0E-1	-(3.66±1.80)E-2
030419	01:12:14.300	(3.78±0.06)E+1	2.0E-1	-(2.81±0.14)E-1
030421	00:36:32.350	(1.27±0.04)E+1	1.0E-1	(8.23±2.40)E-2
030422	09:01:30.850	(1.47±0.11)E+1	3.0E-1	-(3.83±6.08)E-2
030428	22:31:23.300	(9.60±0.26)E+0	2.0E-1	(5.70±1.42)E-2
030501A	01:17:22.300	(7.40±0.49)E+0	2.0E-1	-(2.21±0.55)E-1
030501B	03:10:23.850	(1.17±0.16)E+1	3.0E-1	-(4.00±1.43)E-1
030501C	20:44:49.520	(1.24±0.12)E+0	4.0E-2	(2.21±0.74)E-1
030505A	07:39:13.100	(8.82±0.43)E+1	6.0E-1	(3.77±3.96)E-2
030505B	09:03:26.750	(1.07±0.06)E+2	1.5E+0	-(6.53±4.77)E-2
030506	02:04:27.350	(2.31±0.07)E+1	3.0E-1	-(9.31±2.34)E-2
030518A	01:23:49.650	(2.52±0.02)E+1	1.0E-1	(4.79±0.07)E-1
030518B	03:12:23.050	(1.74±0.12)E+1	3.0E-1	(3.98±0.54)E-1
030519A	09:32:22.700	(3.20±0.39)E+0	2.0E-1	(6.78±1.13)E-1
030519B	14:05:00.100	(9.00±0.21)E+0	2.0E-1	-(1.81±0.47)E-2
030523	14:10:53.190	(1.20±0.26)E-1	2.0E-2	(0.22±1.04)E-1
030528	13:03:07.750	(2.15±0.17)E+1	5.0E-1	-(2.26±0.69)E-1
030601	22:12:06.050	(1.83±0.08)E+1	3.0E-1	(7.59±3.59)E-2
030614	01:30:42.500	(1.68±0.05)E+2	3.0E+0	-(2.19±0.21)E-1
030626	01:46:54.950	(3.85±0.10)E+1	7.0E-1	(2.46±0.18)E-1
030703	19:14:02.400	(5.68±0.74)E+1	8.0E-1	-(0.84±1.03)E-1
030706	00:02:17.750	(4.50±0.45)E+0	3.0E-1	(1.36±0.62)E-1
030710	23:05:02.350	(1.77±0.07)E+1	3.0E-1	-(7.49±0.71)E-1
030714	22:14:50.300	(1.02±0.08)E+1	2.0E-1	-(2.73±0.73)E-1
030716	11:57:19.750	(5.35±0.40)E+1	5.0E-1	-(3.16±0.75)E-1
030721	23:41:10.100	(2.96±0.05)E+1	2.0E-1	(2.88±0.14)E-1
030725	11:46:27.800	(1.84±0.07)E+1	4.0E-1	-(2.22±0.32)E-1
030726A	06:38:41.750	(2.75±0.06)E+1	5.0E-1	(1.56±0.11)E-1
030726B	09:51:37.500	(1.94±0.12)E+2	1.0E+0	-(2.91±0.63)E-1
030728	09:05:55.100	(1.92±0.28)E+1	2.0E-1	(4.26±1.50)E-1
030824	06:31:10.850	(3.00±0.20)E+1	3.0E-1	-(6.11±0.95)E-1
030827	16:08:40.325	(1.85±0.08)E+0	5.0E-2	(7.30±2.77)E-2
030830	18:37:46.250	(2.05±0.09)E+1	5.0E-1	-(1.27±0.34)E-1
030831	15:07:22.450	(2.31±0.09)E+1	3.0E-1	-(1.04±0.33)E-1
030919	21:10:36.750	(2.00±0.14)E+1	5.0E-1	-(2.05±0.59)E-1
030921	08:38:23.650	(1.47±0.06)E+1	3.0E-1	(2.23±3.15)E-2

Table 9. The RHESSI GRB data-set.

GRB	peak time UTC	T_{90} [s]	δt_{res} [s]	hardness ratio log H
030922A	08:43:35.950	(2.28±0.08)E+1	3.0E-1	-(1.07±0.30)E-1
030922B	18:30:56.900	(1.08±0.03)E+1	2.0E-1	(4.63±1.41)E-2
030926	16:52:28.290	(2.80±0.31)E-1	2.0E-2	(2.89±0.77)E-1
031005	08:21:50.250	(1.60±0.18)E+1	5.0E-1	-(4.44±1.19)E-1
031019	22:00:57.175	(7.50±0.71)E+0	1.5E-1	(2.48±0.79)E-1
031024	09:24:14.350	(4.00±0.32)E+0	1.0E-1	(1.77±0.58)E-1
031027	17:07:50.250	(3.90±0.07)E+1	5.0E-1	-(1.03±0.10)E-1
031107	18:24:07.400	(1.92±0.06)E+1	4.0E-1	(1.02±2.13)E-2
031108	14:11:19.250	(2.75±0.07)E+1	5.0E-1	(1.67±0.16)E-1
031111	16:45:20.920	(3.20±0.08)E+0	8.0E-2	(1.50±0.08)E-1
031118	06:26:16.410	(2.60±0.27)E-1	2.0E-2	(2.01±0.57)E-1
031120	05:52:38.250	(9.75±0.30)E+1	1.5E+0	(4.24±2.27)E-2
031127	18:58:55.050	(1.92±0.17)E+1	3.0E-1	-(2.88±0.83)E-1
031130	02:04:53.775	(4.65±0.29)E+0	1.5E-1	(5.52±4.44)E-2
031214	22:50:44.150	(8.30±1.01)E+0	1.0E-1	-(6.98±9.55)E-2
031218	06:28:09.370	(2.20±0.24)E-1	2.0E-2	(1.46±0.51)E-1
031219	05:39:05.850	(7.50±0.21)E+0	1.0E-1	-(1.21±0.21)E-1
031226A	15:43:08.750	(3.45±0.29)E+1	5.0E-1	-(4.63±1.03)E-1
031226B	17:51:29.750	(4.40±0.23)E+1	5.0E-1	-(5.74±4.22)E-2
040102	19:35:26.975	(7.80±0.83)E+0	1.5E-1	-(4.43±1.15)E-1
040108	07:46:39.900	(3.30±0.37)E+1	6.0E-1	-(2.64±1.03)E-1
040113	01:36:46.350	(1.62±0.10)E+1	3.0E-1	-(4.60±5.01)E-2
040115	18:30:11.550	(2.19±0.24)E+1	3.0E-1	-(2.40±0.94)E-1
040125	22:14:47.100	(1.60±0.23)E+1	2.0E-1	-(1.67±1.16)E-1
040205A	05:19:47.350	(3.90±0.62)E+0	1.0E-1	-(2.06±1.29)E-1
040205B	09:27:45.750	(2.65±0.33)E+1	5.0E-1	(2.19±0.98)E-1
040207	22:12:22.600	(2.44±0.06)E+1	4.0E-1	(1.07±0.17)E-1
040211	15:02:08.050	(3.70±0.52)E+0	1.0E-1	-(2.61±1.25)E-1
040215	00:28:02.500	(5.00±0.29)E+1	1.0E+0	-(3.57±0.57)E-1
040220	00:55:15.800	(1.72±0.09)E+1	4.0E-1	(5.71±0.46)E-1
040225A	05:30:53.850	(1.05±0.11)E+1	3.0E-1	-(8.84±8.12)E-2
040225B	10:02:12.200	(1.40±0.16)E+1	4.0E-1	-(3.12±1.10)E-1
040228	00:09:08.500	(2.73±0.02)E+2	2.0E-1	-(1.58±0.07)E-1
040302A	04:14:35.250	(2.37±0.27)E+1	3.0E-1	-(2.76±1.05)E-1
040302B	12:24:03.900	(1.08±0.02)E+1	2.0E-1	-(7.71±0.64)E-2
040303	15:32:37.750	(2.97±0.27)E+1	3.0E-1	-(1.52±0.76)E-1
040312	00:02:36.550	(1.60±0.22)E-1	2.0E-2	(2.13±0.48)E-1
040316	18:16:14.350	(1.50±0.02)E+1	1.0E-1	-(4.87±1.30)E-2
040323	13:03:04.750	(1.89±0.19)E+1	3.0E-1	-(2.92±0.94)E-1
040324	10:21:12.908	(2.55±0.17)E-1	1.5E-2	(2.54±0.26)E-1
040327	16:19:27.500	(2.00±0.32)E+1	1.0E+0	-(4.06±1.54)E-1
040329	11:10:51.965	(2.07±0.04)E+0	3.0E-2	(3.06±0.12)E-1
040330	13:14:42.150	(2.88±0.41)E+1	3.0E-1	(0.04±1.09)E-1
040404	10:58:52.150	(4.90±0.35)E+0	1.0E-1	-(1.38±0.60)E-1
040413	13:09:56.490	(2.80±0.31)E-1	2.0E-2	(1.21±0.68)E-1
040414	11:09:22.500	(7.70±0.24)E+1	1.0E+0	-(1.63±2.36)E-2
040421	02:30:27.300	(1.14±0.02)E+1	2.0E-1	(2.73±0.08)E-1
040423	02:23:30.350	(4.20±0.53)E+0	3.0E-1	-(1.16±0.87)E-1
040425	16:23:34.275	(8.10±0.19)E+0	5.0E-2	(1.08±0.20)E-1
040427	20:12:37.700	(8.00±0.77)E+0	2.0E-1	-(4.55±7.43)E-2
040429	10:53:04.400	(2.52±0.19)E+1	4.0E-1	(2.85±6.00)E-2
040502A	06:37:06.900	(1.86±0.04)E+1	2.0E-1	-(2.97±0.22)E-1
040502B	13:30:02.500	(1.66±0.07)E+2	1.0E+0	-(2.32±0.39)E-1
040506	23:45:18.800	(6.56±0.42)E+1	8.0E-1	-(2.34±0.58)E-1
040508	10:15:44.750	(4.05±0.56)E+1	5.0E-1	-(0.95±1.08)E-1
040510	09:59:37.300	(6.00±0.57)E+0	2.0E-1	-(2.87±0.83)E-1
040513	03:02:17.500	(5.30±0.83)E+1	1.0E+0	-(0.78±1.20)E-1
040526	20:21:13.350	(1.29±0.19)E+1	3.0E-1	-(4.19±1.53)E-1
040528	16:55:58.150	(2.16±0.07)E+1	3.0E-1	-(1.06±0.26)E-1
040531	23:15:04.750	(4.20±0.33)E+1	5.0E-1	-(4.73±0.91)E-1
040601	06:33:24.625	(2.73±0.29)E+1	2.5E-1	(5.10±8.45)E-2
040603A	15:40:58.700	(1.24±0.13)E+1	2.0E-1	-(1.42±0.84)E-1
040603B	19:15:38.500	(7.50±1.00)E+1	3.0E+0	-(5.04±1.49)E-1
040605A	04:31:44.500	(5.80±0.73)E+0	2.0E-1	(3.25±1.04)E-1
040605B	18:46:16.390	(1.80±0.22)E-1	2.0E-2	(2.33±0.48)E-1
040605C	23:58:45.800	(1.68±0.08)E+1	4.0E-1	-(4.30±0.50)E-1

Table 10. The RHESSI GRB data-set.

GRB	peak time UTC	T_{90} [s]	δt_{res} [s]	hardness ratio log H
040611	13:36:00.600	(1.80±0.10)E+1	4.0E-1	(2.02±0.44)E-1
040619	15:15:52.250	(7.70±0.27)E+0	1.0E-1	-(1.74±0.28)E-1
040701	22:46:45.250	(9.60±0.69)E+0	3.0E-1	(9.16±5.34)E-2
040719	01:16:31.250	(7.50±0.65)E+0	1.0E-1	-(1.77±0.73)E-1
040723	04:06:38.150	(1.02±0.04)E+1	1.0E-1	-(1.51±0.27)E-1
040731	10:24:42.750	(2.45±0.07)E+1	5.0E-1	(1.23±0.18)E-1
040803	15:08:57.750	(1.14±0.11)E+2	1.5E+0	-(3.95±1.05)E-1
040810	14:15:42.650	(1.92±0.05)E+1	3.0E-1	-(7.96±1.96)E-2
040818	01:29:04.250	(8.00±0.33)E+0	1.0E-1	(4.57±0.42)E-1
040822	21:21:55.125	(1.38±0.14)E+0	3.0E-2	(2.05±0.83)E-1
040824	05:16:07.500	(4.90±0.50)E+1	1.0E+0	-(4.90±7.92)E-2
040921	16:06:20.265	(2.80±0.73)E-1	7.0E-2	(1.88±0.64)E-1
040925	22:28:59.750	(4.75±0.16)E+1	5.0E-1	(6.66±2.68)E-2
040926	04:03:18.100	(7.60±0.22)E+0	2.0E-1	(1.93±0.11)E-1
041003	09:17:56.250	(9.00±0.74)E+0	5.0E-1	-(1.16±0.52)E-1
041006	12:18:40.350	(1.11±0.08)E+1	3.0E-1	-(4.71±0.80)E-1
041007	02:02:08.350	(2.00±0.13)E+0	1.0E-1	(3.52±0.37)E-1
041009	06:38:21.250	(7.50±0.76)E+0	3.0E-1	-(8.60±7.65)E-2
041010	00:14:57.555	(2.50±0.22)E-1	1.0E-2	(1.58±0.64)E-1
041012	12:40:51.500	(4.60±0.53)E+1	1.0E+0	-(3.90±1.16)E-1
041013A	02:35:25.000	(1.84±0.09)E+2	2.0E+0	(1.27±3.84)E-2
041013B	22:56:27.865	(3.60±0.46)E-1	3.0E-2	(6.92±7.69)E-2
041015	10:22:18.950	(3.90±0.29)E+0	1.0E-1	-(1.82±0.60)E-1
041016	04:39:37.000	(1.80±0.17)E+1	4.0E-1	-(1.90±0.82)E-1
041018	13:08:19.500	(1.02±0.04)E+2	1.0E+0	-(3.19±3.19)E-2
041101	01:49:36.150	(3.20±0.34)E+0	1.0E-1	(2.28±0.85)E-1
041102	11:12:23.750	(2.70±0.22)E+0	1.0E-1	(1.69±0.60)E-1
041107	15:49:29.250	(4.70±0.45)E+1	5.0E-1	-(6.04±7.68)E-2
041116	05:34:56.500	(5.00±0.53)E+1	1.0E+0	-(3.38±1.06)E-1
041117	15:18:00.950	(1.62±0.05)E+1	3.0E-1	-(1.81±0.24)E-1
041120	19:23:41.300	(8.60±0.42)E+0	2.0E-1	-(3.20±0.44)E-1
041125	16:07:27.400	(2.52±0.04)E+1	4.0E-1	-(2.34±0.06)E-1
041202	02:30:57.300	(1.66±0.03)E+1	2.0E-1	(1.14±0.12)E-1
041211A	07:49:56.450	(2.06±0.05)E+1	1.0E-1	-(1.33±0.23)E-1
041211B	11:31:53.400	(2.00±0.09)E+1	4.0E-1	(8.20±3.24)E-2
041211C	23:57:42.925	(6.15±0.16)E+0	1.5E-1	(4.46±0.07)E-1
041213	06:59:36.330	(1.40±0.24)E-1	2.0E-2	(3.19±0.82)E-1
041218	15:45:50.500	(5.10±0.57)E+1	1.0E+0	-(2.22±0.98)E-1
041219	01:42:19.400	(1.00±0.11)E+1	4.0E-1	-(1.32±7.84)E-2
041223	14:06:42.250	(4.05±0.11)E+1	5.0E-1	(8.55±2.11)E-2
041224	20:20:58.250	(3.85±0.58)E+1	5.0E-1	-(3.21±1.42)E-1
041231	21:50:48.050	(1.00±0.12)E+0	1.0E-1	(3.20±0.56)E-1
050124	11:30:03.250	(2.80±0.38)E+0	1.0E-1	-(2.24±1.12)E-1
050126	21:07:37.700	(3.30±0.10)E+1	6.0E-1	-(1.71±0.22)E-1
050203	17:22:00.850	(3.80±0.24)E+0	1.0E-1	-(0.85±4.62)E-2
050213	19:24:04.750	(1.70±0.09)E+1	5.0E-1	(2.43±0.37)E-1
050214	11:38:33.500	(4.00±0.66)E+1	1.0E+0	-(0.16±1.23)E-1
050216	07:26:34.275	(5.00±0.72)E-1	5.0E-2	(5.66±1.00)E-1
050219	21:05:51.650	(9.40±0.17)E+0	1.0E-1	-(3.01±0.15)E-1
050311	17:06:58.850	(2.40±0.44)E+0	3.0E-1	-(1.44±1.09)E-1
050312	05:40:13.575	(1.50±0.51)E-1	5.0E-2	(3.35±0.82)E-1
050314	08:33:08.900	(8.00±0.35)E+0	2.0E-1	-(4.77±0.45)E-1
050320	08:04:26.900	(1.54±0.13)E+1	2.0E-1	(5.51±6.52)E-2
050321	22:11:51.500	(7.00±0.75)E+0	2.0E-1	-(8.21±8.41)E-2
050326	09:53:56.500	(2.70±0.11)E+1	2.0E-1	-(2.54±0.36)E-1
050328	03:25:14.875	(4.50±0.51)E-1	5.0E-2	-(1.02±0.20)E-1
050404	17:27:48.500	(1.14±0.03)E+1	2.0E-1	(1.03±0.18)E-1
050409	01:18:36.050	(1.26±0.05)E+0	2.0E-2	(3.05±0.30)E-1
050411	21:51:09.500	(6.80±0.69)E+0	2.0E-1	-(1.18±0.80)E-1
050412	18:58:45.900	(1.94±0.08)E+1	2.0E-1	-(5.03±0.51)E-1
050429	14:09:50.900	(1.94±0.15)E+1	2.0E-1	(1.35±0.63)E-1
050430	09:13:09.100	(1.42±0.17)E+1	2.0E-1	(0.20±9.23)E-2
050501	08:19:38.825	(2.40±0.19)E+0	1.5E-1	(7.81±4.03)E-2
050502	19:56:57.575	(1.60±0.20)E+0	5.0E-2	(1.61±0.97)E-1
050509	09:31:26.700	(2.00±0.04)E+1	2.0E-1	-(6.35±1.57)E-2
050516	12:58:05.200	(7.60±1.16)E+0	4.0E-1	(1.16±1.11)E-1

Table 11. The RHESSI GRB data-set.

GRB	peak time UTC	T_{90} [s]	δt_{res} [s]	hardness ratio log H
050525A	00:02:54.450	(7.40±0.19)E+0	1.0E-1	-(4.06±0.25)E-1
050525B	00:50:00.500	(1.26±0.03)E+1	2.0E-1	(6.42±1.15)E-2
050528	07:05:23.500	(1.57±0.09)E+2	1.0E+0	-(4.77±0.69)E-1
050530	04:44:44.900	(2.40±0.34)E+0	2.0E-1	(4.69±1.10)E-1
050531	04:27:26.700	(3.32±0.05)E+1	2.0E-1	-(8.44±1.34)E-2
050614	12:02:00.500	(3.10±0.45)E+1	1.0E+0	-(1.73±1.20)E-1
050701	14:22:00.950	(1.00±0.08)E+1	1.0E-1	(2.54±0.69)E-1
050702	07:47:44.160	(1.12±0.16)E+0	8.0E-2	(2.01±1.01)E-1
050703	05:31:50.825	(8.65±0.44)E+0	5.0E-2	-(2.24±0.47)E-1
050706	17:11:37.875	(6.15±0.42)E+0	1.5E-1	-(0.07±5.20)E-2
050713A	04:29:11.750	(1.86±0.07)E+1	3.0E-1	-(9.16±2.81)E-2
050713B	12:07:28.750	(6.05±0.39)E+1	5.0E-1	-(0.35±5.23)E-2
050715	01:15:49.250	(1.14±0.03)E+1	1.0E-1	-(2.32±0.20)E-1
050717	10:30:55.100	(9.60±0.32)E+0	2.0E-1	(2.36±0.23)E-1
050726	20:22:19.800	(1.60±0.06)E+1	4.0E-1	-(5.78±2.30)E-2
050729	01:09:41.120	(4.40±0.47)E+0	8.0E-2	-(8.49±8.47)E-2
050802	10:08:02.850	(2.94±0.31)E+1	3.0E-1	-(1.76±0.90)E-1
050805	13:29:47.625	(1.05±0.08)E+0	5.0E-2	(2.99±0.53)E-1
050809	20:15:26.720	(2.40±0.14)E+0	8.0E-2	-(7.56±3.92)E-2
050813	21:13:43.900	(8.00±0.87)E+0	2.0E-1	(3.68±0.99)E-1
050814	04:35:19.451	(1.24±0.08)E-1	2.0E-3	(6.01±0.64)E-1
050817	10:43:18.900	(2.12±0.20)E+1	2.0E-1	(3.69±0.86)E-1
050820	23:50:36.050	(6.00±0.58)E+0	3.0E-1	-(3.57±0.87)E-1
050824	11:57:42.535	(2.50±0.14)E-1	1.0E-2	(3.31±0.35)E-1
050825	03:34:27.850	(8.00±0.44)E-1	2.0E-2	(1.62±0.42)E-1
050902	12:24:30.650	(1.16±0.10)E+1	1.0E-1	-(5.97±1.18)E-1
050923	01:37:44.850	(9.60±0.56)E+0	1.0E-1	(6.55±4.65)E-2
051009	10:49:02.750	(8.50±0.52)E+1	5.0E-1	-(2.22±0.57)E-1
051012	12:00:11.925	(2.55±0.08)E+0	5.0E-2	(1.14±1.98)E-2
051021	14:01:14.625	(5.10±0.10)E+1	2.5E-1	-(2.26±0.17)E-1
051031	22:01:05.750	(4.95±0.28)E+1	1.5E+0	(4.49±3.88)E-2
051101	01:13:12.625	(1.10±0.14)E+1	1.5E-1	(9.19±9.99)E-2
051103	09:25:42.192	(1.40±0.05)E-1	5.0E-3	(4.68±0.15)E-1
051109	16:42:00.750	(2.55±0.16)E+1	5.0E-1	-(2.15±0.58)E-1
051111	05:59:40.100	(2.38±0.15)E+1	2.0E-1	(1.10±0.53)E-1
051117	12:34:25.300	(3.32±0.13)E+1	2.0E-1	(1.62±0.34)E-1
051119	13:10:59.900	(3.78±0.31)E+1	2.0E-1	-(1.74±0.73)E-1
051124A	08:16:59.450	(1.92±0.15)E+1	1.0E-1	(2.31±0.65)E-1
051124B	14:20:11.100	(3.68±0.19)E+1	2.0E-1	-(2.16±0.48)E-1
051201A	18:31:37.250	(2.25±0.29)E+1	1.5E+0	-(0.50±8.84)E-2
051201B	22:35:30.350	(1.84±0.13)E+1	1.0E-1	(1.29±0.59)E-1
051207	19:04:09.350	(5.73±0.17)E+1	3.0E-1	-(1.75±0.27)E-1
051211	05:28:13.250	(2.94±0.09)E+1	7.0E-1	(1.24±0.17)E-1
051217	09:54:08.650	(1.80±0.27)E+1	3.0E-1	-(0.28±1.14)E-1
051220	13:04:17.525	(1.29±0.01)E+1	5.0E-2	(2.15±0.04)E-1
051220	21:34:36.750	(2.80±0.46)E+1	5.0E-1	-(5.31±2.02)E-1
051221	01:51:15.975	(2.80±0.17)E-1	1.0E-2	(1.65±0.41)E-1
051222	15:07:35.600	(2.44±0.40)E+1	4.0E-1	-(1.73±1.35)E-1
060101	00:34:11.800	(1.96±0.09)E+1	4.0E-1	(6.61±3.35)E-2
060110	08:01:18.900	(1.20±0.16)E+1	2.0E-1	(1.03±1.00)E-1
060111	08:49:00.250	(6.90±0.25)E+1	1.5E+0	(1.61±0.24)E-1
060117	06:50:13.850	(1.59±0.10)E+1	3.0E-1	-(3.13±0.63)E-1
060121A	04:12:56.500	(4.40±0.63)E+1	1.0E+0	(0.17±1.08)E-1
060121B	22:24:56.755	(2.38±0.12)E+0	7.0E-2	-(1.05±0.36)E-1
060123	05:05:24.900	(1.10±0.03)E+1	2.0E-1	-(1.31±0.17)E-1
060124	16:04:22.400	(1.76±0.13)E+1	4.0E-1	(4.99±5.58)E-2
060130	13:48:31.100	(1.52±0.08)E+1	2.0E-1	(2.98±4.17)E-2
060203	07:28:58.535	(5.40±0.45)E-1	1.0E-2	(1.43±0.66)E-1
060217	09:47:43.325	(1.91±0.08)E+1	1.5E-1	-(7.34±3.62)E-2
060224	02:31:11.500	(1.00±0.06)E+1	2.0E-1	-(8.14±4.54)E-2
060228	03:17:33.850	(3.27±0.21)E+1	3.0E-1	-(3.88±5.28)E-2
060303	22:42:47.525	(5.00±0.53)E-1	5.0E-2	(2.56±0.29)E-1
060306	15:22:38.485	(9.20±0.11)E-1	1.0E-2	-(1.07±0.04)E-1
060309	14:38:54.250	(2.95±0.30)E+1	5.0E-1	(1.32±0.81)E-1
060312A	06:17:21.115	(2.40±0.47)E-1	3.0E-2	(2.48±1.16)E-1
060312B	16:44:53.400	(6.80±1.18)E+0	4.0E-1	-(2.32±1.40)E-1

Table 12. The RHESSI GRB data-set.

GRB	peak time UTC	T_{90} [s]	δt_{res} [s]	hardness ratio log H
060313	20:11:32.900	(3.60±0.51)E+0	2.0E-1	(1.52±1.03)E-1
060323	07:04:30.100	(1.76±0.04)E+1	2.0E-1	(3.37±1.52)E-2
060325	12:02:20.350	(1.08±0.02)E+1	1.0E-1	(0.70±1.11)E-2
060401	05:40:18.750	(6.30±0.17)E+0	1.0E-1	(9.21±1.86)E-2
060408	13:11:39.150	(6.90±0.95)E+0	3.0E-1	-(0.06±1.01)E-1
060415	05:31:00.050	(1.32±0.20)E+1	3.0E-1	(1.80±1.14)E-1
060418	03:06:35.800	(4.08±0.21)E+1	4.0E-1	-(1.23±0.43)E-1
060421A	11:03:49.000	(3.12±0.11)E+1	4.0E-1	-(8.58±2.76)E-2
060421B	20:36:38.200	(2.16±0.19)E+1	4.0E-1	-(1.39±0.74)E-1
060425	16:57:38.705	(1.40±0.12)E-1	1.0E-2	(2.59±0.42)E-1
060428	02:30:41.750	(1.35±0.23)E+1	5.0E-1	-(2.45±1.44)E-1
060429	12:19:51.250	(2.00±0.21)E-1	2.0E-2	(2.89±0.33)E-1
060505	23:32:01.050	(9.60±0.46)E+0	3.0E-1	(2.15±0.30)E-1
060528	22:53:05.750	(7.70±0.20)E+1	5.0E-1	(2.41±0.21)E-1
060530	19:19:11.300	(4.00±0.35)E+0	2.0E-1	-(1.16±0.63)E-1
060610	11:22:24.070	(6.00±0.33)E-1	2.0E-2	(2.48±0.38)E-1
060614	12:43:48.250	(5.25±0.45)E+1	1.5E+0	-(1.78±0.72)E-1
060622	17:19:48.750	(2.35±0.09)E+1	5.0E-1	(1.12±0.27)E-1
060624	13:46:56.255	(2.55±0.07)E+0	3.0E-2	-(4.55±0.29)E-1
060625	07:33:27.100	(4.40±0.37)E+0	2.0E-1	(2.21±0.58)E-1
060630	00:06:41.250	(4.10±0.19)E+1	5.0E-1	-(9.96±4.00)E-2
060708	04:30:38.485	(1.14±0.08)E-1	6.0E-3	(1.57±0.36)E-1
060729	04:07:38.600	(5.20±0.53)E+0	2.0E-1	-(1.16±0.79)E-1
060805	14:27:17.450	(5.10±0.07)E+0	6.0E-2	(6.98±0.69)E-2
060811	16:56:43.950	(7.29±0.27)E+1	3.0E-1	-(1.96±0.35)E-1
060819	18:28:20.700	(2.40±0.11)E+1	6.0E-1	(0.84±3.26)E-2
060823	08:05:33.750	(1.00±0.18)E+0	1.0E-1	(3.23±1.26)E-1
060919	21:52:12.750	(2.95±0.37)E+1	5.0E-1	(1.20±0.95)E-1
060920	15:32:38.700	(2.18±0.03)E+1	2.0E-1	(3.59±1.01)E-2
060925	20:14:35.375	(1.65±0.08)E+1	2.5E-1	-(1.00±0.38)E-1
060928	01:20:24.150	(2.03±0.03)E+2	3.0E-1	-(1.28±1.19)E-2
061005	13:38:01.800	(4.24±0.12)E+1	4.0E-1	-(2.05±0.25)E-1
061006A	08:43:39.225	(1.65±0.10)E+0	5.0E-2	(1.53±0.43)E-1
061006B	16:45:27.875	(4.00±0.53)E-1	5.0E-2	(3.23±0.39)E-1
061007	10:08:54.150	(6.06±0.07)E+1	3.0E-1	(1.20±0.08)E-1
061012	11:51:57.850	(9.30±0.48)E+0	1.0E-1	(2.56±0.44)E-1
061013	18:06:28.200	(4.00±0.22)E+1	8.0E-1	-(1.54±0.45)E-1
061014	06:17:02.375	(2.00±0.55)E-1	5.0E-2	(2.56±0.94)E-1
061022	12:23:42.850	(2.19±0.29)E+1	3.0E-1	-(0.44±1.02)E-1
061031	12:19:51.500	(3.30±0.12)E+1	2.0E-1	(7.92±3.06)E-2
061101	21:26:51.550	(1.92±0.30)E+1	3.0E-1	-(2.41±1.40)E-1
061108	01:09:54.850	(3.75±0.09)E+1	3.0E-1	-(8.68±1.90)E-2
061113	13:43:36.050	(1.82±0.03)E+1	1.0E-1	(1.76±0.13)E-1
061117	06:00:11.250	(2.15±0.27)E+1	5.0E-1	(9.86±9.49)E-2
061121	15:23:44.275	(1.46±0.03)E+1	1.5E-1	(1.27±0.17)E-1
061123	16:33:28.650	(5.70±0.32)E+0	1.0E-1	(1.23±0.43)E-1
061126	08:48:03.150	(1.65±0.07)E+1	3.0E-1	(2.49±0.31)E-1
061128	20:01:11.805	(3.00±0.31)E-1	3.0E-2	(3.50±0.27)E-1
061205	05:22:15.450	(7.50±0.91)E+0	3.0E-1	-(1.22±0.96)E-1
061212	05:31:30.970	(1.90±0.01)E+1	6.0E-2	(2.73±0.06)E-1
061222	03:30:19.300	(1.16±0.05)E+1	2.0E-1	(1.44±0.31)E-1
061229	22:25:44.250	(7.95±0.97)E+1	5.0E-1	(1.69±0.93)E-1
061230	23:09:31.000	(2.56±0.19)E+1	8.0E-1	-(1.63±0.60)E-1
070113	11:56:23.815	(2.70±0.48)E-1	3.0E-2	(1.65±1.04)E-1
070116	14:32:16.125	(1.65±0.11)E+1	2.5E-1	(3.79±5.24)E-2
070120	10:48:36.250	(1.85±0.27)E+1	5.0E-1	(1.94±1.07)E-1
070121	10:12:17.000	(8.80±1.60)E+0	8.0E-1	(0.11±1.19)E-1
070125	07:21:27.250	(5.67±0.08)E+1	3.0E-1	(5.03±1.12)E-2
070214	22:39:20.850	(1.77±0.27)E+1	3.0E-1	(1.00±1.11)E-1
070220	04:44:45.300	(2.14±0.11)E+1	2.0E-1	(4.86±4.03)E-2
070221	21:06:46.500	(1.02±0.13)E+1	2.0E-1	-(2.28±9.64)E-2
070307	21:15:43.250	(5.25±0.27)E+1	5.0E-1	-(5.80±4.35)E-2
070402	15:48:39.475	(8.85±0.56)E+0	1.5E-1	(4.96±4.92)E-2
070420	06:18:18.400	(6.16±0.36)E+1	8.0E-1	-(1.63±0.51)E-1
070508	04:18:25.050	(1.31±0.04)E+1	1.0E-1	-(1.71±2.74)E-2
070516	20:41:24.725	(3.50±0.56)E-1	5.0E-2	(5.01±0.73)E-1

Table 13. The RHESSI GRB data-set.

GRB	peak time UTC	T_{90} [s]	δt_{res} [s]	hardness ratio log H
070531	11:45:43.500	(2.60±0.34)E+1	1.0E+0	-(1.08±1.03)E-1
070614	05:05:09.425	(1.50±0.51)E-1	5.0E-2	(3.35±0.64)E-1
070622	02:25:17.850	(1.38±0.03)E+1	1.0E-1	(1.23±0.18)E-1
070626	04:08:44.500	(1.43±0.02)E+2	1.0E+0	(5.00±1.07)E-2
070710	08:22:07.850	(3.90±0.58)E+0	3.0E-1	(0.94±9.91)E-2
070717	21:50:38.750	(1.75±0.20)E+1	5.0E-1	(2.50±0.87)E-1
070722	06:00:31.500	(7.20±0.96)E+0	2.0E-1	(1.02±0.99)E-1
070724	23:25:46.500	(2.40±0.25)E+1	1.0E+0	-(2.08±0.89)E-1
070802	06:16:19.390	(3.12±0.25)E+0	6.0E-2	(4.80±0.78)E-1
070817	14:43:42.250	(8.80±0.71)E+1	5.0E-1	-(9.18±6.84)E-2
070819	10:17:04.750	(3.30±0.26)E+1	5.0E-1	(3.83±6.10)E-2
070821	12:51:31.750	(6.75±0.21)E+1	5.0E-1	(6.03±2.47)E-2
070824	20:50:10.425	(1.30±0.07)E+0	5.0E-2	(1.01±0.29)E-1
070825	01:55:54.250	(3.42±0.09)E+1	3.0E-1	(1.44±0.19)E-1
070917	09:40:31.250	(2.31±0.24)E+1	3.0E-1	(3.20±0.85)E-1
071013	08:53:39.475	(3.65±0.43)E+0	5.0E-2	(3.27±8.94)E-2
071014	03:19:52.450	(7.80±0.37)E+0	1.0E-1	(4.13±3.71)E-2
071030	08:52:41.900	(6.00±0.91)E+0	2.0E-1	(2.20±1.14)E-1
071104	11:41:09.525	(1.47±0.13)E+1	1.5E-1	-(6.66±7.12)E-2
071204	05:58:29.475	(3.00±0.56)E-1	5.0E-2	(3.46±0.72)E-1
071217	17:03:27.950	(8.30±0.48)E+0	1.0E-1	-(9.40±4.89)E-2
080114	16:10:22.300	(7.34±0.07)E+1	2.0E-1	(3.60±0.09)E-1
080202	13:04:37.250	(3.06±0.39)E+1	3.0E-1	(0.15±9.87)E-2
080204	13:56:34.760	(4.88±0.23)E+0	8.0E-2	(4.53±0.42)E-1
080211	07:23:46.250	(2.80±0.08)E+1	5.0E-1	(2.79±0.19)E-1
080218	05:57:28.375	(1.95±0.15)E+1	2.5E-1	(1.18±0.61)E-1
080224	16:58:51.050	(5.40±0.29)E+0	1.0E-1	(2.22±0.41)E-1
080318	08:31:45.050	(1.47±0.16)E+1	3.0E-1	(1.51±0.79)E-1
080319	12:25:56.900	(1.20±0.06)E+1	2.0E-1	(3.29±0.42)E-1
080320	11:52:02.625	(3.05±0.08)E+1	2.5E-1	(1.96±0.22)E-1
080328	08:03:14.500	(8.60±0.62)E+1	1.0E+0	(3.03±0.58)E-1
080330	11:04:33.450	(3.36±0.09)E+1	3.0E-1	(2.54±0.20)E-1
080408	03:36:23.050	(1.40±0.11)E+0	1.0E-1	(5.29±0.37)E-1
080413	08:51:12.250	(7.60±1.20)E+0	1.0E-1	(0.55±1.17)E-1
080425	20:21:47.775	(2.28±0.32)E+1	1.5E-1	(2.58±1.05)E-1